

## Electronic Raman scattering in underdoped $\text{YBa}_2\text{Cu}_3\text{O}_{6.5}$

X. K. Chen, J. G. Naeini, K. C. Hewitt, and J. C. Irwin

*Department of Physics, Simon Fraser University, Burnaby, British Columbia, Canada V5A 1S6*

R. Liang and W. N. Hardy

*Department of Physics, University of British Columbia, Vancouver, British Columbia, Canada V6T 1Z1*

(Received 25 April 1997)

The polarized Raman spectra of underdoped  $\text{YBa}_2\text{Cu}_3\text{O}_{6.5}$  ( $T_c=61$  K) have been measured. The  $XY(B_{2g})$  spectrum exhibits a superconductivity-induced redistribution and a frequency dependence that suggests the presence of nodes near the  $(\pm 1, \pm 1)$  directions in  $k$  space. The  $X'Y'(B_{1g})$  spectrum is unaffected by the transition to the superconducting state and the intensity  $I(B_{1g})$  is significantly reduced relative to the level found in optimally doped compounds. This drop in intensity occurs because of a loss of spectral weight from the regions of the Brillouin zone near  $(\pi, 0)$ , which is associated with the opening of a pseudogap in the underdoped compound. [S0163-1829(97)51426-3]

It is now generally accepted<sup>1</sup> that the superconducting state of the optimally doped high- $T_c$  cuprates is characterized by an anisotropic order parameter with  $d_{x^2-y^2}$  symmetry. This consensus has been reached with the input of different theoretical approaches<sup>1-3</sup> and the results from many different experimental techniques.<sup>4-7</sup> Raman scattering has proved to be valuable in this regard and has provided important contributions<sup>8-12</sup> to the development of the present picture. When interpreted within the conventional model<sup>10-13</sup> of light scattering from a superconductor the polarization dependence of the Raman continua can be used to directly probe the nature of the superconducting order parameter. In particular scattering from selected parts of the Fermi surface (FS) can be studied<sup>12,13</sup> by choosing appropriate scattering geometries. Such experiments, carried out on optimally doped samples, have shown that the peak frequency in the  $B_{1g}$  spectrum, which samples<sup>12</sup> portions of the FS near  $(0, \pm\pi)$  and  $(\pm\pi, 0)$ , provides a measure of the maximum value of the gap. Also, the low frequency behavior of the continua indicates<sup>10</sup> that the superconducting gap has line nodes near the  $(\pm 1, \pm 1)$  directions in the  $k$  space. These features, which are consistent with  $d$ -wave symmetry, are common to several of the optimally doped cuprates.

More recently, attention has shifted to experiments on underdoped and overdoped compounds where the situation is certainly not as clear<sup>14-16</sup> as it is in the optimally doped case. For example, recent angle resolved photoemission (ARPES) experiments<sup>17,18</sup> on underdoped compounds have found that, relative to optimally doped compounds, there is a loss of spectral weight from large regions of the Brillouin zone (BZ) near  $(\pi, 0)$ . It has been suggested that the observed loss of spectral weight from these regions of the BZ is due to the existence of a  $d_{x^2-y^2}$  gap that persists to a temperature  $T^* > T_c$ . Evidence for such a normal state gap has also been obtained using other experimental techniques,<sup>19-21</sup> and it is commonly referred to as a pseudogap. Mechanisms that might lead to the formation of such a pseudogap include the occurrence of precursor pairing<sup>22</sup> without phase coherence,  $d$ -wave pairing of spinons<sup>23,24</sup> at  $T > T_c$  with charge condensation at  $T_c$ , or a Fermi surface depletion<sup>17</sup> caused by a

change in unit cell dimensions induced for example by anti-ferromagnetic correlations. As yet however the origin and nature of the pseudogap are not well understood.

To obtain additional, complementary information on the underdoped phase we have carried out Raman experiments on high quality underdoped  $\text{YBa}_2\text{Cu}_3\text{O}_{6.5}$  single crystals. The effects of underdoping on the scattering intensity, low-frequency behavior, and polarization dependence of the electronic continua have been studied. The low temperature  $B_{2g}$  spectra suggest the presence of an anisotropic gap with nodes. In addition the magnitudes of the measured intensities, relative to those in the optimally doped compounds, can be interpreted in terms of a spectral weight loss that could be associated with the formation of a  $d_{x^2-y^2}$  pseudogap as suggested by photoemission experiments.<sup>17,18</sup> The  $B_{2g}$  intensity measurements also suggest that there is an associated FS evolution, perhaps analogous to that discussed by Chubukov *et al.*<sup>25</sup>

The high quality  $\text{YBa}_2\text{Cu}_3\text{O}_{6.5}$  single crystals used in this study were grown by a flux method in yttrium stabilized zirconia crucibles as described in detail elsewhere.<sup>26</sup> The desired oxygen concentration of the samples was obtained by controlling the annealing conditions.<sup>27</sup> The superconducting transition temperature determined by magnetic susceptibility measurement is 61 K and the transition width is 3 K. The Raman spectra were obtained in a quasibackscattering geometry using the 488 nm and 514.5 nm lines of an Ar-ion laser with an incident intensity of about 20 W/cm<sup>2</sup>. The laser heating effect was estimated to be about 20 K and the temperatures reported in this paper are the resultant temperatures in the excited region of the sample. In the present study, Raman spectra were measured in the  $Z(\overline{XX})\overline{Z}$ ,  $Z(\overline{X'X'})\overline{Z}$ ,  $Z(\overline{XY})\overline{Z}$ ,  $Z(\overline{X'Y'})\overline{Z}$  scattering geometries, where  $X$  and  $Y$  are parallel to the Cu-O bonds and  $X'$  denotes the  $(1,1,0)$  polarization and  $Y'$  the  $(-1,1,0)$  polarization. Considered within the tetragonal point group  $D_{4h}$ , the  $X'Y'$  geometry allows coupling to excitations with  $B_{1g}$  symmetry, the  $XY$  geometry to the  $B_{2g}$  component, and the  $XX$  ( $X'X'$ ) geometry to a combination of the  $A_{1g}$  and  $B_{1g}$  ( $B_{2g}$ ) components.<sup>10</sup>

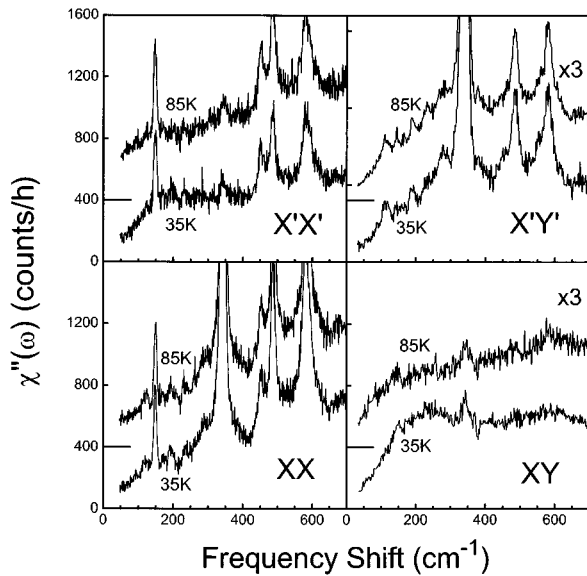


FIG. 1. The Raman response functions ( $\chi''$ ) of  $\text{YBa}_2\text{Cu}_3\text{O}_{6.5}$  obtained at 85 K and 35 K in the  $X'X'(A_{1g}+B_{2g})$ ,  $X'Y'(B_{1g})$ ,  $XX(A_{1g}+B_{1g})$ , and  $XY(B_{2g})$  scattering geometries, which are obtained by dividing the original spectra by the Bose-Einstein thermal factor. The  $XY$  and  $X'Y'$  spectra have been scaled by a factor of 3 to place them on the indicated scale. The 85 K spectra have been displaced upward and the zero level is indicated by the horizontal bar at the left.

The Raman response functions ( $\chi''$ ) for the different scattering geometries, which are obtained by dividing the original spectra by the Bose Einstein factor, are shown in Fig. 1 for the two different temperatures, 85 K ( $T > T_c$ ) and 35 K ( $T < T_c$ ). If we first consider the  $B_{2g}$  spectra shown in the lower right panel of the figure it is evident that there is a superconductivity induced redistribution of the electronic continuum when the sample temperature is lowered below  $T_c$ . In this case  $\chi''(B_{2g})$  increases linearly at small  $\omega$  and a broad gaplike peak, centered at about  $230 \text{ cm}^{-1}$ , appears in the 35 K spectrum. This type of redistribution is qualitatively similar to that observed in spectra obtained from optimally doped compounds.<sup>12,28</sup>

If we now consider the  $X'Y'(B_{1g})$  geometry, we find that the 85 K and 35 K spectra appear to be essentially identical. That is the  $B_{1g}$  spectrum is apparently completely unaffected by the transition to the superconducting state and there is no superconductivity induced redistribution. The low frequency portion ( $\omega < 300 \text{ cm}^{-1}$ ) of  $\chi''(B_{1g})$  increases approximately linearly from the origin in both spectra to intercept the high energy continuum level at about  $200 \text{ cm}^{-1}$ . Although the data are not shown, we have found that this linear behavior at low energies is present in all the  $B_{1g}$  spectra we have obtained for  $35 \text{ K} < T < 290 \text{ K}$ . It should also be noted that we have not found any evidence of peak formation near  $500 \text{ cm}^{-1}$  as observed by Slakey *et al.*,<sup>16</sup> but this could be due to differences in the concentration and/or homogeneity of the oxygen content of the samples.

The spectra obtained in the diagonal geometries appear to parallel the observed behavior of the  $B_{1g}$  (in  $XX$ ) and  $B_{2g}$  (in  $X'X'$ ) spectra. That is, at low energies there does not appear to be a significant  $A_{1g}$  contribution to these spectra and they are dominated by the  $B_{1g}$  and  $B_{2g}$  contributions. A more

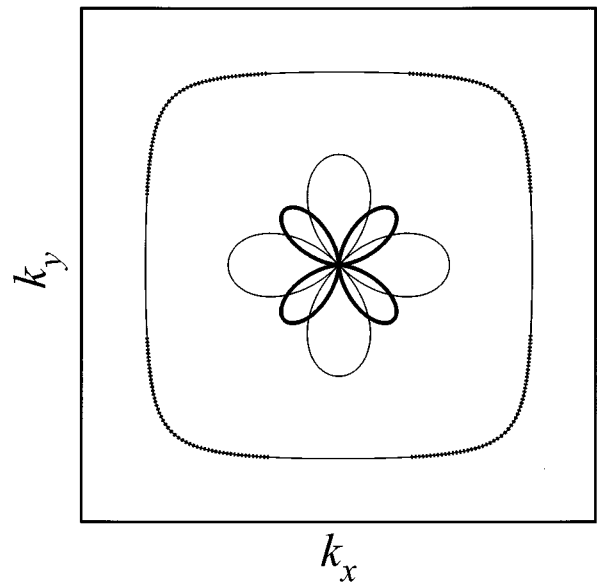


FIG. 2. Schematic illustration of the FS for optimally doped Y123 (solid thin line) and polar plots (see Ref. 28) showing the  $k$  dependence of the magnitude of the  $X'Y'(B_{1g})$  (thin solid line) and  $XY(B_{2g})$  (thick solid line) components of the Raman tensor (1). For a calculation of the spectra in the underdoped compounds (see Fig. 4) it will be assumed that spectral weight is present only on the dashed portions of the FS.

detailed discussion of the spectra and their relative intensities will be presented later in the paper.

For convenience we will discuss our results in terms of the conventional model<sup>10-13</sup> of light scattering from a superconductor. In this model, for nonresonant scattering, the Raman vertex  $\gamma(\mathbf{k})$  can be represented<sup>10-12</sup> by the reciprocal effective mass tensor:

$$\gamma(\mathbf{k}) \propto \hat{\mathbf{e}}^S \cdot \frac{1}{\mu} \cdot \hat{\mathbf{e}}^I = m \sum_{\alpha, \beta} e_{\alpha}^S \frac{\partial^2 \varepsilon(\mathbf{k})}{\partial k_{\alpha} \partial k_{\beta}} e_{\beta}^I, \quad (1)$$

where  $\hat{\mathbf{e}}^S$  and  $\hat{\mathbf{e}}^I$  denote the polarization directions of the scattered and incident light, respectively, and  $\alpha, \beta$  the crystal axes. A spectrum taken in the  $(\alpha\beta)$  scattering geometry (incident light polarized along  $\alpha$  and scattered light along  $\beta$ ) will select the corresponding component of the Raman vertex  $\gamma_{\alpha\beta}(\mathbf{k})$ . It has been shown<sup>10,12,28</sup> that, based on symmetry considerations, the  $B_{1g}(X'Y')$  component and the  $B_{2g}(XY)$  component of the Raman vertex have complementary  $k$  dependence. In particular, the  $B_{1g}$  Raman spectrum samples the FS near the  $(0, \pm 1)$  and  $(\pm 1, 0)$  directions whereas the  $B_{2g}$  spectrum samples a region near the  $(\pm 1, \pm 1)$  diagonals, as illustrated by the polar plot<sup>28</sup> shown in Fig. 2.

Referring again to Fig. 1 we find that the intensities of the  $B_{2g}$  continua at 35 K and 85 K are about the same as the  $B_{1g}$  continua at the same temperatures, which is in direct contrast to what is observed in optimally doped  $\text{YBa}_2\text{Cu}_3\text{O}_x$  where the  $B_{2g}$  continuum is much weaker than the  $B_{1g}$  continuum<sup>29,30</sup> at all temperatures. By comparing with optimally doped samples ( $x = 6.93$ ), we find that as the doping level is reduced to  $x = 6.5$  the  $B_{2g}$  continuum be-

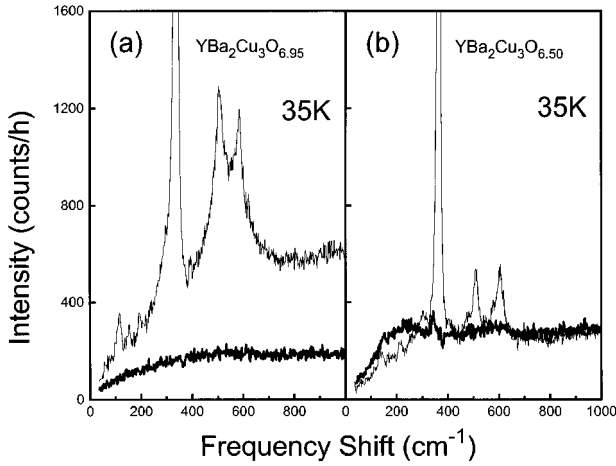


FIG. 3. A comparison of the Raman spectra of Y123 measured in the  $B_{1g}$  (thin lines) and  $B_{2g}$  (bold lines) geometries of (a) optimally doped and (b) underdoped samples.

comes somewhat stronger, whereas the  $B_{1g}$  continuum weakens significantly, and the  $B_{2g}/B_{1g}$  intensity ratio increases by about a factor of about 3 (see Fig. 3). A similar doping dependence in the  $B_{2g}/B_{1g}$  Raman intensity ratio has been recently observed in La214.<sup>31,32</sup> Given the  $k$  dependence of  $\gamma(B_{1g})$  and  $\gamma(B_{2g})$  (Fig. 2) the enhancement of  $\chi(B_{2g})/\chi(B_{1g})$  in the underdoped samples can be understood to be due mainly to a loss of spectral weight from regions of the BZ near  $(\pi,0)$ , which in turn could be associated with the opening of a pseudogap.<sup>17-21</sup> Such a spectral weight loss and an associated  $d_{x^2-y^2}$  (or  $B_{1g}$ ) pseudogap have been found in recent ARPES experiments.<sup>17,18</sup> The reduction in strength of the  $B_{1g}$  continuum that we have observed here is thus in accord with this aspect of the ARPES measurements.

To illustrate these considerations we can use the conventional model of light scattering<sup>13</sup> to produce a schematic representation of the spectra. The unscreened response function is given by<sup>13</sup>

$$\chi''(q=0,\omega) \sim \frac{1}{\omega} \left\langle \frac{|\gamma(\mathbf{k})|^2 |\Delta(\mathbf{k})|^2}{(\omega^2 - 4|\Delta(\mathbf{k})|^2)^{1/2}} \right\rangle, \quad (2)$$

where  $\langle \dots \rangle$  denotes an average over the FS with the restriction that  $\omega > 2|\Delta(\mathbf{k})|$ . The results shown in Fig. 4 were obtained with  $\Delta(k) = \Delta_0(\cos k_x a - \cos k_y a)$  and a second neighbor tight binding model with parameters used previously.<sup>29</sup> The spectra obtained by integrating (2) over the full FS (Fig. 2) are indicated by solid lines in Fig. 4. Assume now that all the spectral weight is lost from regions of the FS near  $(\pi,0)$  which are represented by the solid lines portions of the FS shown in Fig. 2. To obtain a representation of the spectra in the underdoped case we then restrict the integration in Eq. (2) to the portions of the FS shown by the dashed lines (Fig. 2). In this case we obtain the spectra shown by the heavy dashed lines in Fig. 4. It is clear from this schematic illustration that a loss of spectral weight in regions near the axes could result in a situation where the  $B_{1g}$  and  $B_{2g}$  spectra have approximately equal strengths. This picture is, of course, overly simplistic and does not take into account

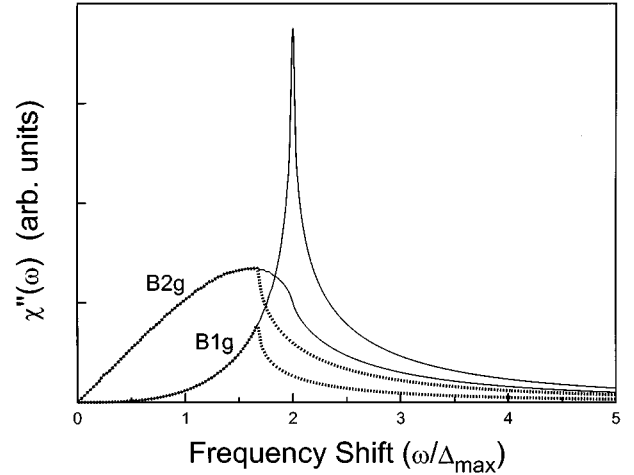


FIG. 4. Calculated  $B_{1g}$  and  $B_{2g}$  Raman response functions (solid lines) obtained by integrating over the full FS of Fig. 2 and the modified response functions (heavy dashed lines) obtained by restricting the integration to the dashed region of the FS in Fig. 2.

changes in the band structure that might occur<sup>17</sup> and which would be required to explain the observed enhancement of the  $B_{2g}$  response function in the underdoped compound. In this regard the present results can also be understood qualitatively in terms of a FS evolution, analogous to that discussed by Chubukov *et al.*<sup>25</sup> or observed in ARPES.<sup>17</sup>

Since the  $B_{2g}$  spectrum (Fig. 1) is the only one that is sensitive to the transition to the superconducting state it is the only geometry that can be used to gain information on the symmetry of the superconducting gap. Fortunately, however, among all the investigated scattering geometries,  $B_{2g}$  is the most important for testing the  $d_{x^2-y^2}$  gap symmetry since the  $B_{2g}$  Raman spectrum samples the FS near the  $(\pm 1, \pm 1)$  diagonals where the gap nodes might be located. If one expands  $\gamma$  and  $\Delta$  in the integration in Eq. (2) for angles near the diagonal directions one finds that  $\chi''(B_{2g})$  should increase linearly with  $\omega$ . Since the low temperature  $B_{2g}$  spectrum in Fig. 1 exhibits a linear frequency dependence at low temperature, the presence of the nodes along the diagonal directions is suggested.<sup>10</sup> The magnitude of the superconducting gap ( $\Delta_{\max}$ ) is of course also of interest but since the  $B_{1g}$  spectrum is not sensitive to  $T_c$  we cannot obtain  $\Delta_{\max}$  directly from the spectra. Also  $\omega(B_{2g})$  cannot be used in this regard since it could be influenced (Fig. 4) by the nature and magnitude of the pseudogap or the mechanism responsible for the observed redistribution of spectral weight.

From Fig. 1 it is evident that the  $B_{1g}$  response function rises linearly at low energies. The origin of this linear increase is not clear. It is tempting to use this feature of the  $B_{1g}$  spectrum to speculate on the nature of the mechanism responsible for the observed loss of spectral weight. It must be remembered, however, that the low-energy portion of the  $B_{1g}$  continuum could be altered by the presence of the strong  $B_{1g}$  phonon and scattering contributions from the chains.<sup>33</sup> These aspects could be responsible for the low energy linear dependence that appears to be observed at all doping levels.<sup>14</sup> On the other hand, disorder<sup>34</sup> and the orthorhombic distortion in Y123 (Ref. 35) can also produce a linear  $B_{1g}$  response at low frequencies even in the presence of a

$d$ -wave gap. In view of these comments the observed linear dependence of the  $B_{1g}$  spectrum cannot be used to rule out  $d$ -wave symmetry for the normal state gap.

Finally both the  $X'X'$  and  $XX$  spectra at 35 K also exhibit a linear dependence at low energies. Although the  $A_{1g}$  spectra might increase<sup>11</sup> linearly in the presence of a  $d$ -wave gap, we can note that in the present case the  $A_{1g}$  components of the spectra are also significantly reduced because of the effective depletion of the FS. Thus, as is suggested by the spectra, the low energy portion of the  $XX$  and  $X'X'$  spectra in Fig. 1 appear to be dominated by the  $B_{1g}$  and  $B_{2g}$  contributions and hence do not provide additional information. It should also be noted that the simple model used to obtain Fig. 4 also yields results<sup>32</sup> that are in qualitative agreement with this statement and the spectra shown in Fig. 1.

In summary, the  $B_{2g}/B_{1g}$  intensity ratio of the Raman continua in underdoped  $\text{YBa}_2\text{Cu}_3\text{O}_{6.5}$  at temperatures above and below  $T_c$  is found to be approximately three times as large as that in the optimally doped  $\text{YBa}_2\text{Cu}_3\text{O}_{6.93}$ , which is attributed to a loss of spectral weight, or FS depletion, in the  $(\pm\pi, 0)$  and  $(0, \pm\pi)$  regions of the BZ. This depletion could result from the presence of a  $d_{x^2-y^2}$  pseudogap.<sup>17-19</sup> The low-frequency linear behavior of the  $B_{2g}$  spectrum at temperatures below  $T_c$  indicates the existence of line nodes in the superconducting gap near the  $(\pm 1, \pm 1)$  diagonals, which is consistent with the gap having  $d_{x^2-y^2}$  symmetry.

The authors would like to thank Dr. T. P. Devereaux and Dr. G. A. Sawatzky for helpful discussions. The financial support of the Natural Sciences and Engineering Council of Canada is gratefully acknowledged.

- 
- <sup>1</sup>J. Annett, N. Golgenfeld, and A. J. Legget, in *Physical Properties of High Temperature Superconductors V*, edited by D. M. Ginsburg (World Scientific, Singapore, 1996).
- <sup>2</sup>P. Monthoux, A. Balatsky, and D. Pines, Phys. Rev. Lett. **67**, 3448 (1991); Phys. Rev. B **46**, 14 803 (1992).
- <sup>3</sup>N. E. Bickers, D. J. Scalapino, and S. R. White, Phys. Rev. Lett. **62**, 961 (1989).
- <sup>4</sup>W. N. Hardy *et al.*, Phys. Rev. Lett. **70**, 3999 (1993).
- <sup>5</sup>Z. X. Shen *et al.*, Science **267**, 343 (1995).
- <sup>6</sup>D. A. Wollman *et al.*, Phys. Rev. Lett. **71**, 2134 (1993).
- <sup>7</sup>J. R. Kirtley *et al.*, Nature (London) **373**, 225 (1995).
- <sup>8</sup>R. Hackl *et al.*, in *Spectroscopic Studies of Superconductors*, edited by I. Bozovic and D. van der Marel (SPIE, Bellingham, 1996).
- <sup>9</sup>T. Staufer *et al.*, Phys. Rev. Lett. **68**, 1069 (1992).
- <sup>10</sup>T. P. Devereaux *et al.*, Phys. Rev. Lett. **72**, 396 (1994).
- <sup>11</sup>T. P. Devereaux and D. Einzel, Phys. Rev. B **51**, 16 336 (1995).
- <sup>12</sup>X. K. Chen *et al.*, J. Supercond. **7**, 435 (1994); Physica C **227**, 113 (1994).
- <sup>13</sup>M. V. Klein and S. B. Dierker, Phys. Rev. B **29**, 4976 (1984).
- <sup>14</sup>X. K. Chen *et al.*, Phys. Rev. B **48**, 10 530 (1993).
- <sup>15</sup>C. Kendziora and A. Rosenberg, Phys. Rev. B **52**, R9867 (1995).
- <sup>16</sup>F. Slakey *et al.*, Phys. Rev. B **42**, 2643 (1990).
- <sup>17</sup>D. S. Marshall *et al.*, Phys. Rev. Lett. **76**, 4841 (1996); A. G. Loeser *et al.*, Science **273**, 325 (1996).
- <sup>18</sup>H. Ding *et al.*, Nature (London) **382**, 51 (1996); H. Ding *et al.*, Phys. Rev. Lett. **78**, 2628 (1997).
- <sup>19</sup>J. W. Loram, K. A. Mirza, and J. R. Cooper, Phys. Rev. Lett. **71**, 1740 (1993).
- <sup>20</sup>W. W. Warren *et al.*, Phys. Rev. Lett. **62**, 1193 (1989).
- <sup>21</sup>A. V. Puchkov *et al.*, Phys. Rev. Lett. **77**, 3212 (1996).
- <sup>22</sup>S. Kivelson and V. Emery, Nature (London) **374**, 434 (1995).
- <sup>23</sup>G. Kotliar and J. Liu, Phys. Rev. B **38**, 5142 (1988); P. W. Anderson, Science **235**, 1196 (1987).
- <sup>24</sup>X. G. Wen and P. A. Lee, Phys. Rev. Lett. **76**, 503 (1996).
- <sup>25</sup>A. V. Chubukov *et al.* (unpublished).
- <sup>26</sup>Ruixing Liang *et al.*, Physica C **195**, 51 (1992).
- <sup>27</sup>P. Schleger *et al.*, Physica C **176**, 261 (1991).
- <sup>28</sup>X. K. Chen *et al.*, Phys. Rev. Lett. **73**, 3290 (1994).
- <sup>29</sup>X. K. Chen and J. C. Irwin, Physica C **235-240**, 1089 (1994).
- <sup>30</sup>M. Krantz and M. Cardona, J. Low Temp. Phys. **99**, 205 (1995); D. Reznik *et al.*, Phys. Rev. B **48**, 7624 (1993).
- <sup>31</sup>J. G. Naeini *et al.* (unpublished).
- <sup>32</sup>X. K. Chen *et al.* (unpublished).
- <sup>33</sup>A. Secuto *et al.*, Solid State Commun. **85**, 589 (1993).
- <sup>34</sup>T. P. Devereaux, Phys. Rev. Lett. **74**, 4313 (1995).
- <sup>35</sup>T. Strohm and M. Cardona, Phys. Rev. B **55**, 12 725 (1997).